

## ■ Non-Planar Aromatics

## Compressing a Non-Planar Aromatic Heterocyclic [7]Helicene to a Planar Hetero[8]Circulene

Bodil Lousen,<sup>[a]</sup> Stephan K. Pedersen,<sup>[a]</sup> Pernille Bols,<sup>[a]</sup> Kasper H. Hansen,<sup>[a]</sup> Michelle R. Pedersen,<sup>[a]</sup> Ole Hammerich,<sup>[a]</sup> Sergey Bondarchuk,<sup>[b]</sup> Boris Minaev,<sup>[b]</sup> Glib V. Baryshnikov,<sup>[c]</sup> Hans Ågren,<sup>[c, d]</sup> and Michael Pittelkow\*<sup>[a]</sup>

**Abstract:** This work describes a synthetic approach where a non-planar aromatic heterocyclic [7]helicene is compressed to yield a hetero[8]circulene containing an inner antiaromatic cyclooctatetraene (COT) core. This [8]circulene consists of four benzene rings and four heterocyclic rings, and it is the first heterocyclic [8]circulene containing three different heteroatoms. The synthetic pathway proceeds via a the flattened dehydro-hetero[7]helicene, which is partially a helicene and partially a circulene: it is non-planar and helically chiral as helicenes, and contains a COT motif like [8]circulenes. The antiaromaticity of the COT core is confirmed by nucleus independent chemical shift (NICS) calculations. The planarization from a helically  $\pi$ -conjugated [7]helicene to a fully planar heterocyclic [8]circulene significantly alters the spectroscopic properties of the molecules. Post-functionalization of the [7]helicenes and the [8]circulenes by oxygenation of the thiophene rings to the corresponding thiophene-sulfones allows an almost complete fluorescence emission coverage of the visible region of the optical spectrum (400–700 nm).

Helicenes are aromatic compounds in which angularly *ortho*-annulated rings ultimately form a stereogenic axis. Helicenes exist as all-benzene molecules and as heterocyclic compounds, in which one or more benzene rings are replaced with heterocycles such as furans, thiophenes and pyrroles.<sup>[1]</sup> These intrinsi-

cally chiral molecules have found vast applications in such diverse fields as molecular recognition, catalysis and detection or emission of circularly polarized light.<sup>[2–5]</sup> Structurally related motifs to the [*n*]helicenes are the [*n*]circulenes. These structures also consist of *ortho*-annulated aromatic rings, but instead forms a cyclic structure, having a central ring with *n* sides. It is illustrative to view the all-benzene series of [*n*]circulenes, which consists of the bowl-shaped carba[5]circulene (corannulene), the planar carba[6]circulene (coronene) and the saddle-shaped [7]- and [8]circulenes. Hetero[8]circulenes incorporating four five-membered heterocycles (furans, pyrroles, thiophenes) are planar,<sup>[6,7]</sup> and these structures can be viewed as containing antiaromatic cyclooctatetraene (COT) cores. [*n*]Circulenes may also, instead of being viewed as two annulenes connected by single bonds, be viewed as [*n*]radialenes, which are *n*-membered rings with *n* exocyclic double bonds. The difference between being an [*n*]circulene and an [*n*]radialene, where each end of the exocyclic double bonds is connected by an etheno-bridge or a heteroatom, is formally a discussion of resonance structures.

The first tetrahetero[8]circulenes were prepared by Erdtman and Högberg during their studies of the oligomerization of substituted benzoquinones **1**. This yielded the tetraoxa[8]circulenes **2**, via a Lewis acid mediated tetramerization (Figure 1 top).<sup>[8]</sup>

Inspired by this work we reported that 3,6-dihydroxycarbazoles **3**, upon treatment with chloranil and boron trifluoride diethyl etherate, can be dimerized into the corresponding diazadioxal[8]circulenes **4** which contain two pyrroles (Figure 1 top). The introduction of four pyrroles was accomplished by Osuka and co-workers by an oxidative “fold-in” fusion reaction of a tetrapyrrole compound **5** providing tetraaza[8]circulene **6** (Figure 1 top).<sup>[9]</sup> Recently also strategies for introduction of thiophene has been described.<sup>[10]</sup>

In this work, we describe how diazathia[7]helicene **7** can be converted into the intermediary dehydro[7]helicene **8** and diazaoxathia[8]circulene **9** by a sequential annulation protocol (Figure 1 bottom). The dehydro[7]helicene resembles both the hetero[8]circulene and the hetero[7]helicene by having a cyclooctatetraene motif incorporated into a near helical structure. The hetero[8]circulene **9** contains one thiophene, one furan and two pyrroles, and is the first compound in the hetero[8]circulene family to include three different heterocycles.<sup>[11]</sup> Incorporation of thiophene allows for convenient oxygenation and the preparation of the closely related sulfones **7-SO<sub>2</sub>**, **8-SO<sub>2</sub>**

[a] B. Lousen, Dr. S. K. Pedersen, P. Bols, K. H. Hansen, M. R. Pedersen, Prof. O. Hammerich, Prof. M. Pittelkow  
Department of Chemistry, University of Copenhagen  
Universitetsparken 5, 2100 Copenhagen Ø (Denmark)  
E-mail: pittel@chem.ku.dk

[b] Dr. S. Bondarchuk, Prof. B. Minaev  
Department of Chemistry and Nanomaterials Science  
Bohdan Khmelnytsky National University, 18031 Cherkasy (Ukraine)

[c] Dr. G. V. Baryshnikov, Prof. H. Ågren  
Division of Theoretical Chemistry and Biology  
School of Engineering Sciences in Chemistry, Biotechnology and Health  
KTH Royal Institute of Technology, 10691, Stockholm (Sweden)

[d] Prof. H. Ågren  
College of Chemistry and Chemical Engineering  
Henan University, Kaifeng, Henan 475004 (P. R. China)

 Supporting information and the ORCID identification number(s) for the author(s) of this article can be found under:  
<https://doi.org/10.1002/chem.201905339>

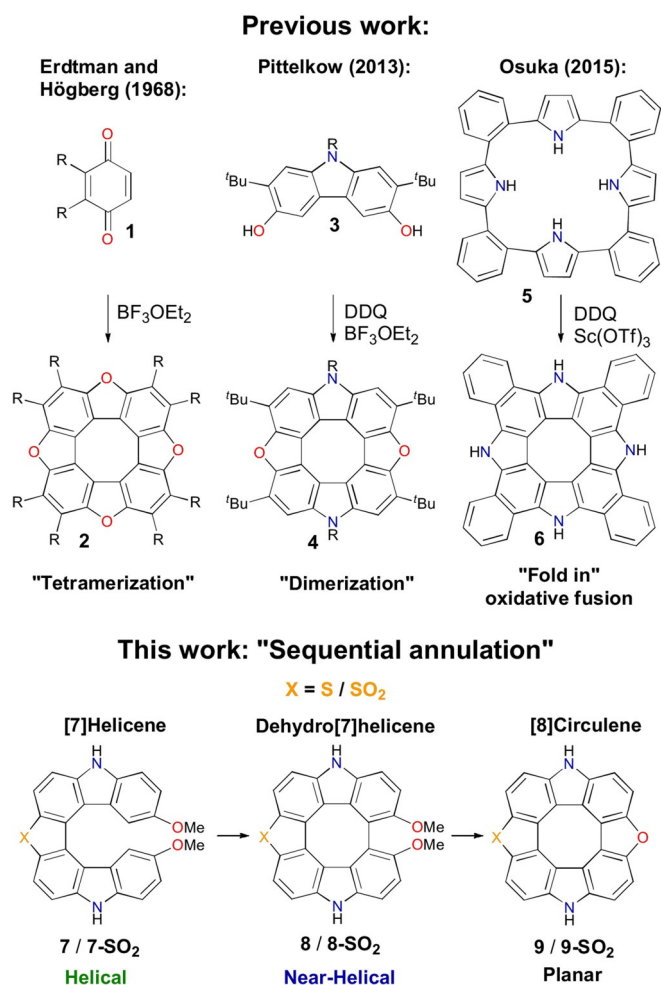
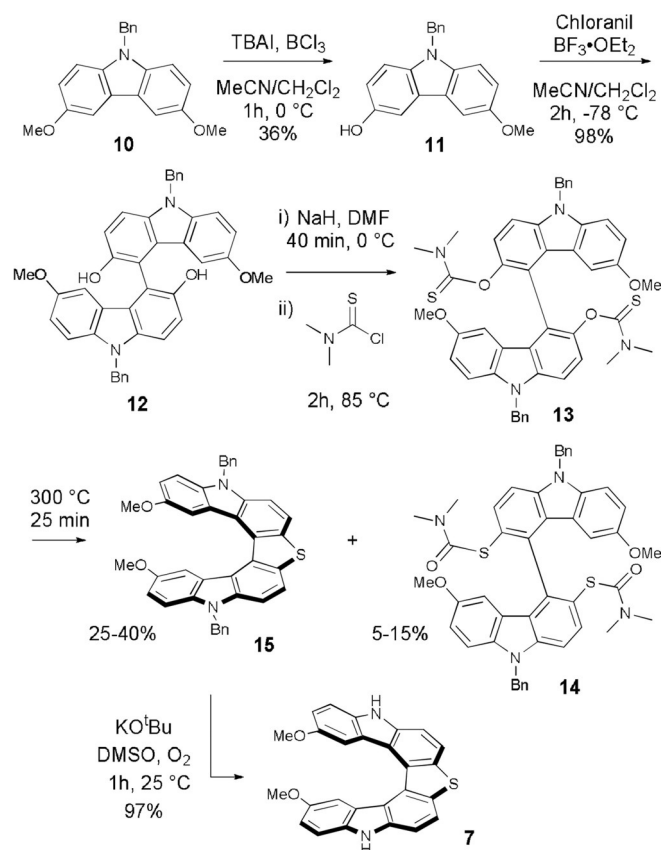


**Figure 1.** Top: Overview of previously reported strategies for synthesis of hetero[8]circulenes. Bottom: This work: Synthesis of a hetero[8]circulene by a sequential annulation strategy.

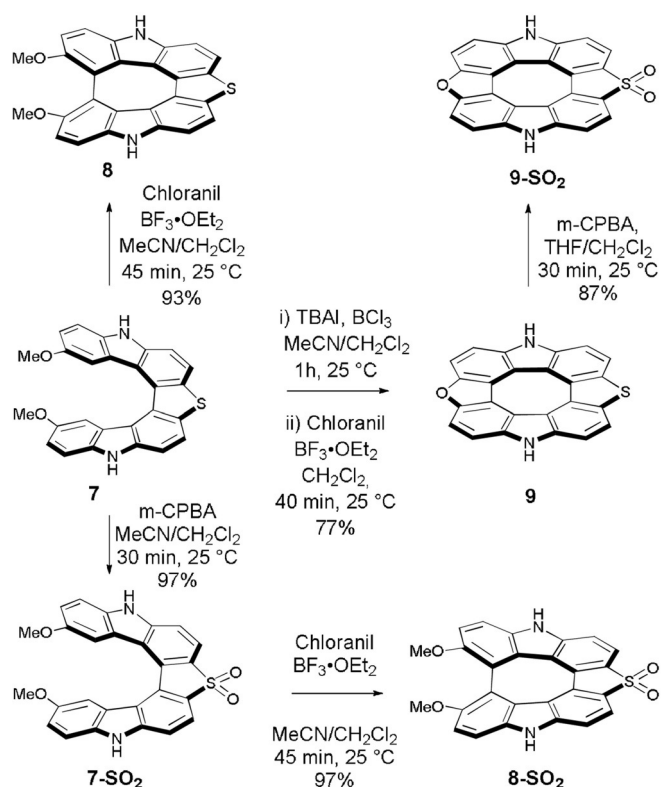
and 9-SO<sub>2</sub>. Sequential annulation and oxygenation are found to be an efficient method for tuning the optical properties. Both annulation and oxygenation cause a bathochromic shift in absorbance as well as emission. Together, the compounds emissions cover almost the entire visible spectrum. Computational experiments predict that the dehydro[7]helicenes **8** and **8-SO<sub>2</sub>** have higher racemization barriers than the parent [7]helicenes **7** and **7-SO<sub>2</sub>**. NICS calculations show significant paratropic and antiaromatic character in both the COT motifs are present in the dehydro[7]helicenes **8** and **8-SO<sub>2</sub>** and in the [8]circulenes **9** and **9-SO<sub>2</sub>**.

Thiadiaza[7]helicene **7** was synthesized in five steps from 3,6-dimethoxy-carbazole **10** (Scheme 1).<sup>[6]</sup> Mono-demethylation of **10** to **11** was followed by dimerization into bicarbazolediol (BICOL, **12**) in 95% yield by an oxidative coupling reaction mediated by chloranil and BF<sub>3</sub>·OEt<sub>2</sub>, with complete regioselectivity for the 4,4'-coupled product. This high degree of regioselectivity is a significant improvement to the previous reported synthesis of BICOL motifs.<sup>[12,13]</sup> Omission of BF<sub>3</sub>·OEt<sub>2</sub> did not result in conversion, and increasing the temperature above 0 °C, resulted in a loss of regioselectivity due to formation of



**Scheme 1.** Preparation of diazaoxathia[7]helicene (**7**).

the 2,4'-coupled isomer (for more details see Supporting Information). Interestingly, no formation of furan by oxidative dehydration was observed, despite this being the major product for 2,7-di-*tert*-butyl analogues of hydroxycarbazole **11**.<sup>[6,14]</sup> To install the annulating thiophene heterocycle, attention was turned to the thermal Newman-Kwart rearrangement reaction, which has proven useful in synthesis of thia[*n*]helicenes from biaryllic 2,2'-Newman-Kwart substrates (bis-*O*-arylthiocarbamates).<sup>[19]</sup> Heating bis-*O*-arylthiocarbamate (**13**) at 300 °C for 25 minutes gave both the rearranged product (**14**) and the diaza[7]helicene (**15**). Under optimized conditions, the [7]helicene **15** was isolated in 40% yield. Debenzylation of [7]helicene **15**, using DMSO and KOtBu under an oxygen atmosphere, provided thiadiaza[7]helicene (**7**) in 97% yield.<sup>[15]</sup> With the [7]helicene (**7**) in hand, its derivatization to a variety of oxidation products was explored (Scheme 2). Treatment with BF<sub>3</sub>·OEt<sub>2</sub> and chloranil gave the cyclodehydrogenated dehydro[7]helicene (**8**) quantitatively in an intramolecular Scholl type reaction.<sup>[16,17]</sup> Demethylation using BCl<sub>3</sub> and TBAI, before treatment with BF<sub>3</sub>·OEt<sub>2</sub> and chloranil, severely changes the reactivity, enabling furan formation via an oxidative dehydration reaction, providing diazaoxathia[8]circulene (**9**). For further derivatization, oxidation of the thiophene heterocycles into their corresponding sulfones was explored. Oxidation with *m*-CPBA, gave the corresponding sulfones (**7-SO<sub>2</sub>**, **8-SO<sub>2</sub>** and **9-SO<sub>2</sub>**, Scheme 2).



**Scheme 2.** Preparation of [7]helicene (7- $\text{SO}_2$ ), dehydro[7]helicenes (8 and 8- $\text{SO}_2$ ), and circulenes (9 and 9- $\text{SO}_2$ ) from diazaoxathia[7]helicene (7).

To understand the structural effects of intramolecular oxidative coupling and the subsequent annulation, the geometries of the compounds were investigated. As numerous attempts of growing crystals of sufficient quality for single-crystal X-ray diffraction have failed, the geometry of structures of the compounds were calculated using the B3LYP/6-31+G(d) method. From the data (Figure 2) it is clear that the oxidative cyclodehydrogenation of [7]helicenes (7 and 7- $\text{SO}_2$ ) into dehydro[7]helicenes (8 and 8- $\text{SO}_2$ ) changes the geometry of the structures

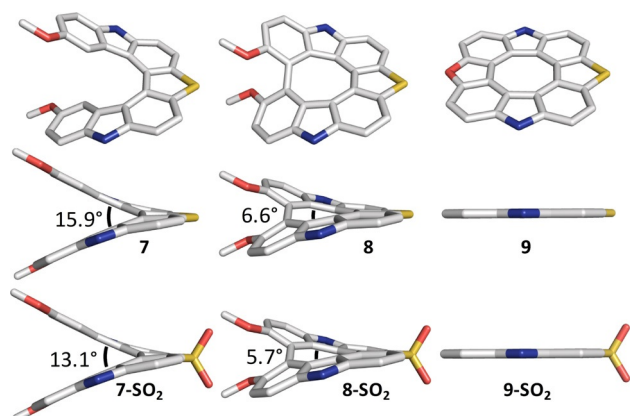


**Figure 2.** Structures of prepared compounds 7, 7- $\text{SO}_2$ , 8, 8- $\text{SO}_2$ , 9 and 9- $\text{SO}_2$  and bite-angles obtained by the B3LYP/6-31+G(d) method. The sequential annulation protocol causes planarization of the structures reflected by decrease in dihedral angle.

dramatically, as the termini of the helicene are forced towards each other, which inherently causes some planarization of the molecules. This is reflected in the inner dihedrals of the compounds, which decrease from 15.9° to 6.6° when going from 7 to 8 and from 13.1° to 5.7° when going from 7- $\text{SO}_2$  to 8- $\text{SO}_2$ . The methoxy substituents preclude complete planarization in the dehydro[7]helicenes (8 and 8- $\text{SO}_2$ ), whereas the furans introduced in 9 and 9- $\text{SO}_2$  allows for planarization of the [8]circulenes (9 and 9- $\text{SO}_2$ ). The planarity of these heterocyclic [8]circulenes is consistent with what has previously been observed for related hetero[8]circulenes.<sup>[11]</sup>

The optical properties of the series were investigated by UV/Vis and fluorescence spectroscopy in THF (Figure 3). Looking first at the effect of planarization of the motif, it is observed that going from the [7]helicene (7) through dehydro[7]helicene (8) to the planar [8]circulene (9), cause a red-shift in the onset of absorption. This is consistent with the expected effect upon increasing the extent of conjugation.<sup>[18,19]</sup> Focusing on the effect of oxygenation to the electron-withdrawing sulfone, a redshift of around 40 nm (ca. 2000  $\text{cm}^{-1}$ ) for each of the three compounds was observed. This demonstrates the advantage of introducing thiophenes in the aromatic system, as it allows for tuning the HOMO–LUMO gap of the presented compounds. Focusing on the effect on fluorescence spectra, the

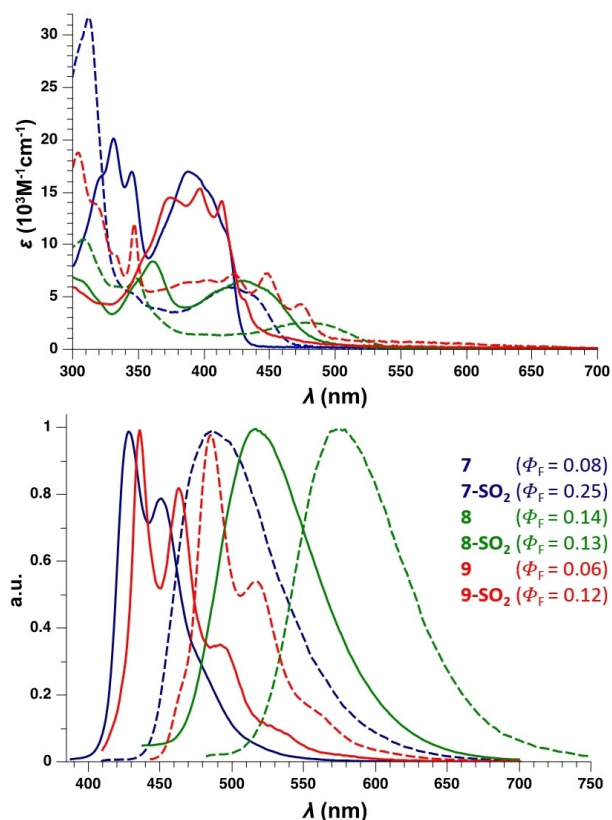


**Figure 3.** UV/Vis absorption (top) and emission spectra (bottom) of compounds 7 (solid blue lines), 7- $\text{SO}_2$  (dashed blue lines), 8 (solid green lines), 8- $\text{SO}_2$  (dashed green lines), 9 (solid red lines) and 9- $\text{SO}_2$  (dashed red lines) in THF. Quantum yields were measured using 9,10-diphenylanthracene as standard. The series covers almost fully the visible spectrum.

same trend was observed, that is, a bathochromic shift from planarization, and likewise by oxidation to sulfone. By using these simple synthetic modifications presented (planarization and oxygenation), the emission of the presented compound class covers the majority of the visible spectrum (ca. 400–700 nm), albeit only with moderate fluorescence quantum yields (0.08–0.25).

The electrochemical properties of the compounds were investigated using cyclic voltammetry and differential pulse voltammetry (Table 1). Only the dehydro[7]helicenes (**8** and **8-SO<sub>2</sub>**) showed reversible oxidations. From the first oxidation of the series of [7]helicenes, the dehydro[7]helicenes and the [9]circulenes it is apparent that the sulfones (**7-SO<sub>2</sub>**, **8-SO<sub>2</sub>** and **9-SO<sub>2</sub>**) are more difficult to oxidize than their corresponding sulfides (**7**, **8** and **9**). The first oxidation potential for the [8]circulenes (**9** and **9-SO<sub>2</sub>**) are comparable to previously determined oxidation potentials for diazadioxo[8]circulenes (0.63–0.67 V),<sup>[14]</sup> tetraoxa[8]circulenes (0.72–1.10 V),<sup>[25]</sup> and azatrioxa[8]circulenes (0.65–0.67 V).<sup>[26]</sup>

Compound	<b>7</b>	<b>7-SO<sub>2</sub></b>	<b>8</b>	<b>8-SO<sub>2</sub></b>	<b>9</b>	<b>9-SO<sub>2</sub></b>	<b>15</b>
ox1 [V]	0.40	0.70	0.33	0.46	0.57	0.64	0.50

Both the [7]helicenes (**7** and **7-SO<sub>2</sub>**) and the dehydro[7]helicenes (**8** and **8-SO<sub>2</sub>**) comprise intrinsic axial chirality and hence the ability to racemize thermally. Unsuccessful attempts of resolving **7**, **7-SO<sub>2</sub>**, **8** and **8-SO<sub>2</sub>** using HPLC analysis with chiral stationary phases (columns of LUX cellulose type from Phenomenex were tested, in different solvent systems MeCN/MeOH/H<sub>2</sub>O mixtures with 0.1% HCOOH or TFA) indicate that the compounds racemize rapidly at room temperature or that we simply have not identified an appropriate combination of stationary and mobile phase to achieve these separations.

The difficulty of this type of separation has previously been reported for helicenes of similar size.<sup>[20,21]</sup> It is disappointing that our efforts towards resolving the enantiomers of the [7]helicenes and the dehydro[7]helicenes failed, as applications of optically pure helicene-based fluorophores in light-emitting devices is an attractive research area. We have, in unpublished work, prepared analogues of the [7]helicenes (**7**) in which the sulfur atoms are replaced with oxygen atoms, and in those molecules the barrier to racemization is in the range of 50 °C. The oxygen analogue did not have methoxy groups, but larger alkoxy groups, which is expected to give rise to a higher racemization barrier. This indicates to us that the racemisation barrier in **7** and **8** will also be in that range, or lower. At this stage we cannot, however, distinguish between the two scenarios: 1) the racemisation barrier is below room temperature even though calculations suggest it should not be, and 2) our HPLC methods used in resolving experiments were unsuited.

To investigate the effect of the cyclodehydrogenation on the transition states and the racemization barriers of, respectively,

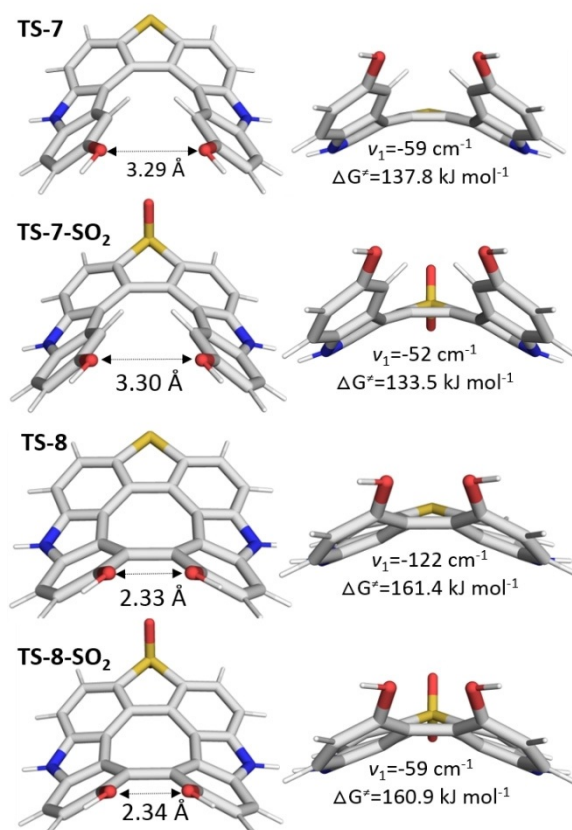


**Figure 4.** Calculated transition state structure and the energy barriers for racemization processes. Dehydrohelicenes (**8** and **8-SO<sub>2</sub>**) have higher barriers than helicenes (**7** and **7-SO<sub>2</sub>**). Sulfone analogues have slightly lower barriers.

the [7]helicenes (**7** and **7-SO<sub>2</sub>**) and the dehydro[7]helicene (**8** and **8-SO<sub>2</sub>**), attention was turned to DFT calculations. For both the [7]helicenes and the dehydro[7]helicenes, saddle-shaped transition states for racemization were obtained (Figure 4). The result shows larger racemization barriers for the cyclodehydrogenated compounds (**8** and **8-SO<sub>2</sub>**), than for the [7]helicenes (**7** and **7-SO<sub>2</sub>**) (161.4 and 160.9 kJ mol<sup>-1</sup> vs. 137.8 and 133.5 kJ mol<sup>-1</sup>). These observations are in contrast to Osuka's investigation of a similar but unsubstituted couple of a triaza[7]helicene and a dehydro-triaza[7]helicene, in which a planar transition state, with a lowered barrier, was predicted for the dehydro[7]helicene.<sup>[20]</sup> The difference in transition states can be rationalized by the two methoxy groups **8** and **8-SO<sub>2</sub>** have in the 2- and 2'-positions, as these, due to their size, precludes the formation of a planar transition state.<sup>[20]</sup> In the saddle-shaped transition states, the distance between the substituents at the 2- and 2'-positions is crucial for the size of the barrier, as increased repulsion between the substituents increases the energies and the racemization barriers. This explains why the cyclodehydrogenated structures (**8** and **8-SO<sub>2</sub>**), where the distance between the methoxy groups is around 1 Å smaller than for the [7]helicenes (**7** and **7-SO<sub>2</sub>**) (3.30–3.29 Å vs. 2.33–2.34 Å), have higher barriers. The oxygenation to sulfone has very little effect on the racemization barriers.

Comparing our calculated energy barriers with those of the calculated barriers of Osuka's molecules, and the fact that Osuka has reported to have successfully resolved one of the three dehydro-triaza[7]helicenes reported indicate that our molecules (**7** and **8**) should indeed be possible to resolve into the enantiomers.<sup>[20]</sup>

It has been shown previously that the planar central ring in hetero[8]circulenes possess large positive NICS(0,1)-values attributed to the antiaromatic nature of the planar COT.<sup>[22,23]</sup> Formally four of the compounds in the presented series contain  $8\pi$ -electron inner rings, namely the dehydro[7]helicenes (**8** and **8-SO<sub>2</sub>**) and circulenes (**9** and **9-SO<sub>2</sub>**). Only the circulenes have planar COTs and they show positive NICS(0)-values in the eight-membered central rings, of, respectively, 7.73 ppm for **9** and 8.50 ppm for **9-SO<sub>2</sub>** (Figure 5). Also the slightly non-planar central rings of the dehydro[7]helicenes (**8** and **8-SO<sub>2</sub>**) show positive NICS(0)-values of, respectively, 7.63 for **8** and 7.41 ppm for **8-SO<sub>2</sub>**, thus slightly less positive than for the completely planarized circulenes (**9** and **9-SO<sub>2</sub>**), but still clearly suggesting that the structures share the paratropic and antiaromatic nature of the inner COT of circulenes despite the non-planar geometry in dehydro[7]helicenes. To rule out the possibility that the positive NICS(0) values of the central eight-membered ring in the dehydro[7]helicenes are a consequence of the proximity to the surrounding aromatic rings, a computa-

tional control experiment calculating the NICS(0)-values in the central axis of the helicenes (which does not contain a central COT) were performed (Figure 5 b). Five points along the central axis of the helicenes were examined in which the NICS indices were found to be considerably positive, meaning that a paratropic ring current also exists inside the helix. This can be explained in terms of so-called induced paratropicity which sometimes is observed in partially saturated circulenes.<sup>[24]</sup>

The [7]helicenes (**7** and **7-SO<sub>2</sub>**) and the dehydrohelicenes (**8** and **8-SO<sub>2</sub>**) all possess global diatropic clockwise ring currents in their outer conjugated circuit. These currents change direction to counter-clockwise, when moving to the inner circuit, as schematically shown in Figure 5 c, thereby inducing paratropicity inside the helices. In the case of hetero[8]circulenes **9** and **9-SO<sub>2</sub>**, which are fully annulated circulenes, the "annulene-with-annulene" model is valid. This enables the existence of two almost independent current flows: a paratropic current in the COT core and a diatropic current outside in the outer perimeter (Figure 5 c). The "annulene-with-annulene" model has previously proven valid for various hetero[8]circulenes including the species **2** and **4**.<sup>[23,24]</sup> Thus, one can say that planar hetero[8]circulenes should be generally viewed as two annulenes connected by single bonds rather than as  $[n]$ radialenes.

In summary, the first antiaromatic heterocyclic [8]circulene with three different heterocycles have been synthesized using a novel synthetic sequential annulation strategy, in which heterocyclic [7]helicenes are planarized. From computational studies, racemization barriers for [7]helicene and dehydro[7]helicene have been estimated and the role of edge substituents on these barriers has been established. Topologically induced paratropicity has been predicted for the [7]helicene and dehydro[7]helicene molecules, whereas the "annulene-with-annulene" model is valid for the [8]circulenes. Effects of derivatization of the thiophene have been explored in this work, and investigation of further derivatization of the pyrroles are ongoing in our laboratory.

## Conflict of interest

The authors declare no conflict of interest.

**Keywords:** chirality • helicenes • non-planar aromatics • structure/property relations • synthetic methodology

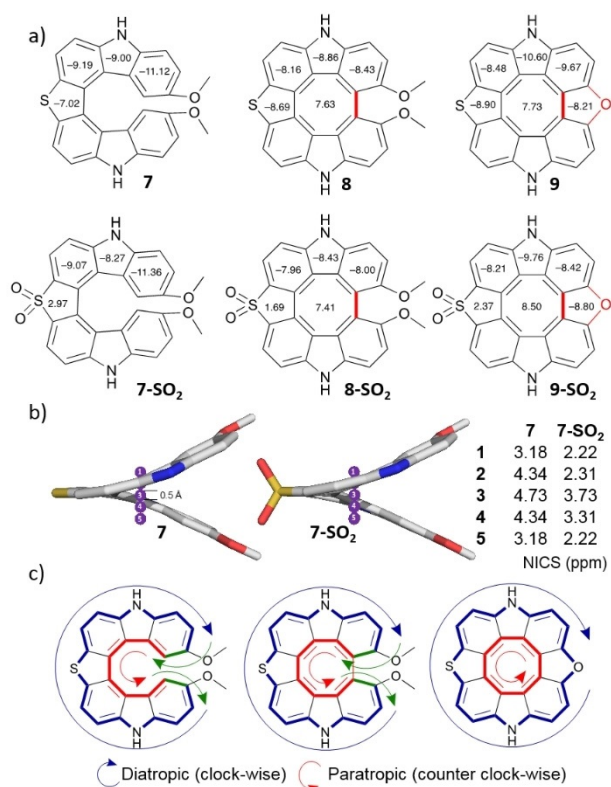


**Figure 5.** NICS(0)-values (ppm). a) The NICS indices for compounds calculated in the centre of each five-, six- and eight-membered ring. b) Ring-current topologies in helicene **7**, dehydrohelicene **8** and circulene **9**. c) The NICS indices for helicenes **7** and **7-SO<sub>2</sub>** calculated along the main axis with the step of 0.5 Å, by the B3LYP/6-311++G(d,p) method in GIAO approximation.

[1] a) Y. Shen, C.-F. Chen, *Chem. Rev.* **2012**, *112*, 1463–1535; b) H. Hopf, *Chem. Rec.* **2014**, *14*, 979–1000; c) K. Dhbaibi, L. Favereau, J. Crassous, *Chem. Rev.* **2019**, *119*, 8846–8953.

[2] K. Shinohara, Y. Sannohe, S. Kaieda, K. Tanaka, H. Osuga, H. Tahara, Y. Xu, T. Kawase, T. Bando, H. Sugiyama, *J. Am. Chem. Soc.* **2010**, *132*, 3778–3782.

[3] M. R. Crittall, H. S. Rzepa, D. R. Carbery, *Org. Lett.* **2011**, *13*, 1250–1253.

[4] Y. Yang, R. C. da Costa, M. J. Fuchter, A. J. Campbell, *Nat. Photonics* **2013**, *7*, 634–638.

[5] Y. Yang, R. C. da Costa, D. M. Smilgies, A. J. Campbell, M. J. Fuchter, *Adv. Mater.* **2013**, *25*, 2624–2628.

[6] a) T. Hensel, D. Trpcevski, C. Lind, R. Grosjean, P. Hammershøj, C. B. Nielsen, T. Brock-Nannestad, B. E. Nielsen, M. Schau-Magnussen, B. Minaev, G. V. Baryshnikov, M. Pittelkow, *Chem. Eur. J.* **2013**, *19*, 17097–17102; b) C. B. Nielsen, T. Brock-Nannestad, P. Hammershøj, T. K. Reenberg, M.

- Schau-Magnussen, D. Trpceviski, T. Hensel, R. Salcedo, G. V. Baryshnikov, B. F. Minaev, M. Pittelkow, *Chem. Eur. J.* **2013**, *19*, 3898–3904.
- [7] K. Y. Chernichenko, V. V. Sumerin, R. V. Shpanchenko, E. S. Balenkova, V. G. Nenajdenko, *Angew. Chem. Int. Ed.* **2006**, *45*, 7367–7370; *Angew. Chem.* **2006**, *118*, 7527–7530.
- [8] H.-E. Högborg, *Acta Chem. Scand.* **1972**, *26*, 2752–2758.
- [9] F. Chen, Y. S. Hong, S. Shimizu, D. Kim, T. Tanaka, A. Osuka, *Angew. Chem. Int. Ed.* **2015**, *54*, 10639–10642; *Angew. Chem.* **2015**, *127*, 10785–10788.
- [10] a) X. Xiong, C.-L. Deng, Z. Li, X.-S. Peng, H. N. C. Wong, *Org. Chem. Front.* **2017**, *4*, 682–687; b) S. Kato, S. Akahori, Y. Serizawa, X. Lin, M. Yamau-chi, S. Yagai, T. Sakurai, W. Matsuda, S. Seki, H. Shinokubo, Y. Miyake, *J. Org. Chem.* **2020**, *85*, 62–69.
- [11] T. Hensel, N. Andersen, M. Plesner, M. Pittelkow, *Synlett* **2015**, *26*, 498–525.
- [12] P. N. M. Botman, M. Postma, J. Fraanje, K. Goubitz, H. Schenk, J. H. van Maarseveen, H. Hiemstra, *Eur. J. Org. Chem.* **2002**, 1952.
- [13] J. Brussee, A. C. A. Jansen, *Tetrahedron Lett.* **1983**, *24*, 3261–3262.
- [14] S. Pedersen, K. Eriksen, M. Pittelkow, *Angew. Chem. Int. Ed.* **2019**, *58*, 18419–18423; *Angew. Chem.* **2019**, *131*, 18590–18594.
- [15] A. A. Haddach, A. Kelleman, M. V. Deaton-Rewolinski, *Tetrahedron Lett.* **2002**, *43*, 399–402.
- [16] L. Zhai, R. Shukla, R. Rathore, *Org. Lett.* **2009**, *11*, 3474–3477.
- [17] M. Grzybowski, K. Skonieczny, H. Butenschön, D. T. Gryko, *Angew. Chem. Int. Ed.* **2013**, *52*, 9900–9930; *Angew. Chem.* **2013**, *125*, 10084–10115.
- [18] G. Bidan, A. De Nicola, V. Enée, S. Guillerez, *Chem. Mater.* **1998**, *10*, 1052–1058.
- [19] K. Nakanishi, D. Fukatsu, K. Takaishi, T. Tsuji, K. Uenaka, K. Kuramochi, T. Kawabata, K. Tsubaki, *J. Am. Chem. Soc.* **2014**, *136*, 7101–7109.
- [20] a) F. Chen, T. Tanaka, T. Mori, A. Osuka, *Chem. Eur. J.* **2018**, *24*, 7489–7497; b) Y. Matsuo, F. Chen, K. Kise, T. Tanaka, A. Osuka, *Chem. Sci.* **2019**, *10*, 11006–11012.
- [21] M. Hasan, A. D. Pandey, V. N. Khose, N. A. Mirgane, A. V. Karnik, *Eur. J. Org. Chem.* **2015**, 3702–3712.
- [22] G. V. Baryshnikov, B. F. Minaev, M. Pittelkow, C. B. Nielsen, R. Salcedo, *J. Mol. Model.* **2013**, *19*, 847–850.
- [23] G. V. Baryshnikov, R. R. Valiev, N. N. Karaush, B. F. Minaev, *Phys. Chem. Chem. Phys.* **2014**, *16*, 15367–15374.
- [24] G. V. Baryshnikov, R. R. Valiev, V. N. Cherepanov, N. N. Karaush-Karmazin, V. A. Minaeva, B. F. Minaev, H. Ågren, *Phys. Chem. Chem. Phys.* **2019**, *21*, 9246–9254.
- [25] C. B. Nielsen, T. Brock-Nannestad, T. K. Reenberg, P. Hammershøj, J. B. Christensen, J. W. Stouwdam, M. Pittelkow, *Chem. Eur. J.* **2010**, *16*, 13030–13034.
- [26] M. Plesner, T. Hensel, B. E. Nielsen, F. S. Kamounah, T. Brock-Nannestad, C. B. Nielsen, C. G. Tortzen, O. Hammerich, M. Pittelkow, *Org. Biomol. Chem.* **2015**, *13*, 5937–5943.

---

Manuscript received: November 25, 2019

Revised manuscript received: February 9, 2020

Accepted manuscript online: February 13, 2020

Version of record online: March 20, 2020